Simulation of Peak Stresses and Bowing Phenomena during the Cool Down of a Cryogenic Transfer System

Hubertus Tummescheit[†], Kristian Tuszynski[†] , Philipp Arnold[‡]
Modelon AB[†], Ideon Science Park, SE-22370 Lund, Sweden
Linde Kryotechik AG[‡], CH-8422 Pfungen, Switzerland
Hubertus.Tummescheit@modelon.se, Kristian.Tuszynski@modelon.se

Abstract

An extension for cryogenic systems to the AirConditioning Library by Modelon was used to analyze the cool down of a cryogenic transfer system where Linde Kryotechnologie in Pfungen, Switzerland was the main contractor. Simulation was used early in the design process to make sure that the system was well designed for a number of cool-down scenarios. Early detection of problematic parts of the system for some cool-down sequences lead to changes in the piping design. Simulation was also used to assess the maximum thermal stresses during cool down and determine suitable mass flow rates. Proper cool-down sequences were established iteratively with the help of a combined simulation of the cryogenic two-phase flow, the heat conduction in solid structures and the resulting thermal stresses. The two main problems to avoid during cool down are (1) excessive thermal stresses in thick-walled components, and (2) bowing of pipes with liquid cryogen in the lower part of a long, horizontal pipe with gaseous cryogen above. Two similar systems where considered, one for liquid hydrogen, the other for liquid oxygen. Dymola and Modelica were choosen for the project due to the good multi-domain and multi-physics capabilities, and the availability of model libraries that covered a large part of the problem.

Keywords: Cryogenics, two-phase flow, transient thermal stress simulation

1 Introduction

The Indian Space Research Organization, ISRO, is building and commissioning a new cryogenic engine test rig in their Liquid Propulsion Test Centre in Mahendragiri, Tamil Nadu. The system under investigation is the cryogenic transfer system for the cryogenic fluids hydrogen and oxygen, used to transfer cryogen from tankers into the run-tanks and from both tankers and run tanks to the test objects. The system is designed for a wide range of pressures and flow rates which leads to a rather complex overall structure of pipes, valves and measurement equipment. Simulations of the system cool down was used early in the design process to validate the design – here the main issue is to avoid bowing of dead-end pipes – and to find improvement potential from an operational point of view. Simulation was also used later on to establish suitable cool-down flow rates and valve sequences that fulfill the two main requirements: use as little cryogen as possible for cool down while not exceeding the maximum allowed thermal stresses.

Obtaining the desired mass flow rates in a transient two-phase flow system throughout the system is very difficult because of the enormous change in densities between gaseous and liquid cryogen: the density ratio can be up to 1:1000. During the filling of the system with liquid, deviations between local mass flow rates and controlled rates at a valve with one-phase inlet conditions can be large. In the situations when the control valve is inside the two-phase region, actual mass flow rates can not be controlled at all.

2 Modeling of thermal stress in cylindrical bodies

The model for thermal stress is based on a radial discretization of cylindrical geometries both for pipes and valves. For the bowing phenomenon, also a tangential discretization and, if necessary an axial one are added. The energy balance of a cylindrical slice of the pipe is based on the Fourier equation with a central difference approximation of the temperature gradient and takes the temperature dependence of the heat capacity and thermal conductivity into account. Stresses are computed separately for the stress introduced through temperature gradients and the mechanical stress due to the pressure inside the pipe. The stress vectors are summed to compute a total equivalent stress. The equivalent stress reaches its

maximum value either on the inside of the cylinder or on the outside of the cylinder. The ratio of the maximum equivalent stress and the yield stress is the *stress ratio*.

The Fourier equation is given by [7],

$$\frac{\rho_i}{\lambda_i}\left(\frac{\partial T_i}{\partial t} Cp_i + \frac{\partial Cp_i}{\partial t} T_i\right) = A_i \cdot T_{i-1} + B_i \cdot T_i + C_i \cdot T_{i+1} \quad (1)$$

Where *i = 2, 3.. Nr-1* and *Nr* is the discretization number of the material in radial direction. The two remaining elements are given by the boundary conditions.

The calculation of the Fourier coefficients, *A*, *B* and *C* for a radial discretization is shown in equation *(2)*.

$$A_i = \frac{r_i + r_{i-1}}{r_i (r_i - r_{i-1})(r_{i+1} - r_{i-1})}$$

$$B_i = \frac{r_{i+1} + r_i}{r_i (r_{i+1} - r_i)(r_{i+1} - r_{i-1})} \quad (2)$$

$$C_i = -A_i - B_i$$

The axial heat conduction in the material is assumed to be negligible.

To obtain the thermal stress distribution, three stress components in tangential (Θ), radial (r) and axial (z) directions are calculated. The general stress equations are given by

$$\sigma_\theta = \frac{E \cdot \alpha}{(1-\nu) r^2} \cdot \left[\frac{r^2 + r_i^2}{r_o^2 + r_i^2} \int_{r_i}^{r_o} T(r)\, r\, dr + \int_{r_i}^{r} T(r)\, r\, dr - T(r) \cdot r^2 \right]$$

$$\sigma_r = \frac{E \cdot \alpha}{(1-\nu) r^2} \cdot \left[\frac{r^2 - r_i^2}{r_o^2 + r_i^2} \int_{r_i}^{r_o} T(r)\, r\, dr - \int_{r_i}^{r} T(r)\, r\, dr \right]$$

$$\sigma_z = \frac{E \cdot \alpha}{(1-\nu)} \cdot \left[\frac{2}{r_o^2 + r_i^2} \int_{r_i}^{r_o} T(r)\, r\, dr - T(r) \right] \quad (3)$$

where *E* is the Young modulus, *α* the linear expansion coefficient and *υ* the Poisson ratio.

By only calculating the thermal stress at the inner and outer points of the wall (the maximum stress of a pipe is always at one of these points) the equations can be simplified as:

$$\begin{aligned} \sigma_\theta^i &= \frac{E_1 \cdot \alpha_1}{(1-\nu_1)} \cdot \left[Tm - T(r_i) \right] \\ \sigma_\theta^o &= \frac{E_{Nr} \cdot \alpha_{Nr}}{(1-\nu_{Nr})} \cdot \left[Tm - T(r_o) \right] \\ \sigma_z^i &= \frac{E_1 \cdot \alpha_1}{(1-\nu_1)} \cdot \left[Tm - T(r_i) \right] \\ \sigma_z^o &= \frac{E_{Nr} \cdot \alpha_{Nr}}{(1-\nu_{Nr})} \cdot \left[Tm - T(r_o) \right] \\ \sigma_r^i &= 0, \qquad \sigma_r^o = 0 \end{aligned} \quad (4)$$

Where *Tm* is the mean temperature of the material and 1 and Nr refer to the innermost and outermost radial discretizations respectively.

The effective stress according to Von-Mises theory results in (from [7]):

$$\sigma_{eff} = \sqrt{\sigma_\theta^2 + \sigma_z^2 + \sigma_r^2 - (\sigma_\theta \cdot \sigma_r + \sigma_\theta \cdot \sigma_z + \sigma_r \cdot \sigma_z)} \quad (5)$$

The stress-ratio is defined as the ratio of effective stress to yield stress of the material:

$$\sigma_{ratio} = \frac{\sigma_{eff}}{\sigma_Y} \quad (6)$$

The two different problems analyzed later in the paper need different discretizations.

1. The thermal stress analysis from cool-down requires a two-dimensional model with radial and axial discretizations to capture the local thermal stresses along the pipe.
2. The bowing problem requires axial and tangential discretizations to capture the different deformations on the top and bottom of a pipe where the bottom is filled with boiling liquid and the top is filled with saturated gas.

Both cases were captured with a single model with all 3 discretizations, where the ones that were not needed were set to one element.

3 Flow modeling

For the two-phase flow in the pipes, a standard finite volume method assuming homogeneous equilibrium flow was used as described in [2] and [3]. Due to the partially violent transients, a dynamic momentum balance has been used for some of the simulations. Heat transfer needs to take into account the „sub-cooled boiling" regime, which is important towards the end of the cool down and is present during a large fraction of the overall cooldown time. Pressure drop models are from the standard literature like [4]. Properties for oxygen were implemented according to [1], hydrogen properties according to [8], and the results were compared to RefProp by NIST which contains the same property models.

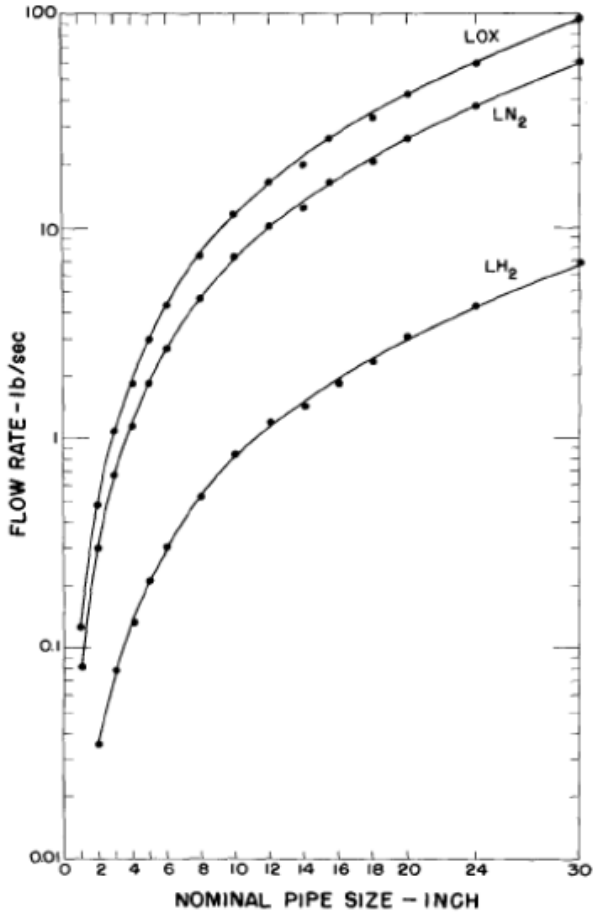

Figure 1: Flow rate which predicts non-stratified flow conditions for pipeline fluid qualities below95% (liquid and gas phase assumed saturated at boiling point), from [9].

The main trade-off that has to be taken into account is between minimal cryogen consumption for cool-down and a minimal cool down time. The mass flow is restricted by an upper limit, usually determined by the maximum allowable thermal stress, and a lower limit. The lower limit is defined by the „non-stratified flow" condition. A stable phase separation with liquid flow on the bottom of the pipe and gaseous flow above it results in differences in the heat transfer rate of about one order of magnitude. They may lead to faster cooldown on the bottom of the pipe, which may lead to bowing. The limit for stratified flow conditions for cryogens has been investigated in [9].

It could be argued that a homogeneous equilibrium model does not capture the physics of the cool down flow sufficiently accurate. For the main focus of the study, the thermal stress in the thick-walled components, it is not necessary to predict the flow and the flow-regime exactly (appart from avoiding stratified flow conditions), and therefore we do not believe that a non-homogeneous flow would improve the quality of the results in a way that would justify the much higher model complexity.

4 Low temperature properties

Both the thermal conductivity and the heat capacity of metal pipes go to 0 at 0 degrees Kelvin. This has a

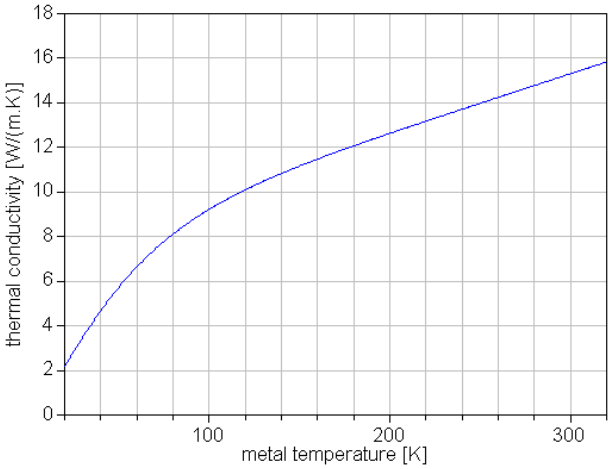

Figure 2: Thermal conductivity for steel 316L as a function of temperature.

number of surprising effects when the temperatures are approaching the lower limits (ca. 20 K for liquid hydrogen and ca. 80 K for liquid oxygen): the cold parts of metal pipes and valves almost insulate the remaining warmer parts from the cryogen, effectively slowing down the last part of the cool down.

Fortunately detailed data for metals used in cryogenic transfer systems is publicly available from NIST (National Institute for Standards and Technology) via their web-based database, see [8].

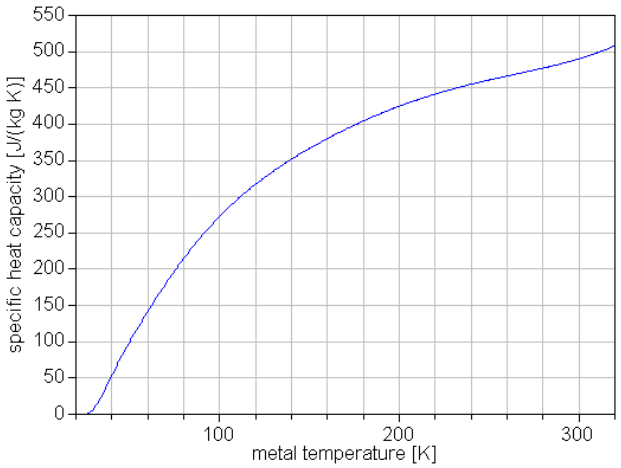

Figure 3: Specific heat capacity for steel 316L as a function of temperature.

5 Thermal stress results

For the evaluation of thermal stresses, a 10 m long pipe with ca 150 mm diameter (DN 150) and ca 8 mm wall thickness, material stainless steel 316 for oxygen and 304 for hydrogen, directly downstream of an open-close valve that opens completely in 2 seconds is investigated. The results for pipes give a good understanding for the situation of the complete system as they demonstrate well the differences caused by the different cryogen properties The upstream properties are:

1. Liquid oxygen of 0.5 MPa at 91 K.
2. Liquid hydrogen of 0.5 MPa at 21 K.

In both cases, the highest stress is not directly down stream of the valve but a short distance into the pipe, at a location where the combination of high heat transfer coefficient and large ΔT results in the combination with the highest heat flow. The longitudinal discretization is 20 segments, the radial discretization 10 segments for pipes.

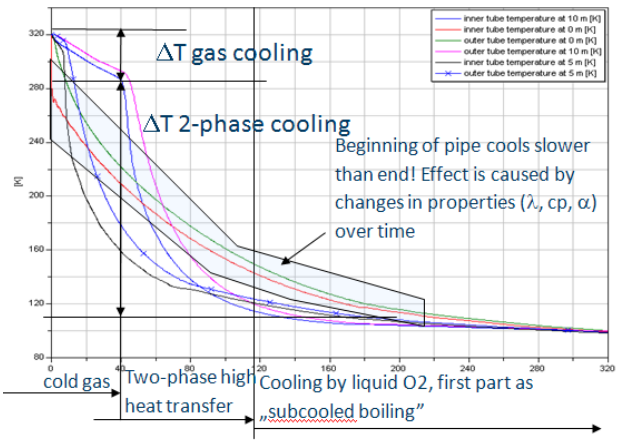

Figure 4: Temperature over time with different phases for a 10m high-pressure pipe during cool down with an oxygen mass flow of 1.7 kg/s at control valve.

Different phases of cooldown can be clearly distinguished from the temperature trajectories. The difference between hydrogen and oxygen cool down is also striking, but becomes understandable once the influences of the different thermophysical properties of the fluids and the metals are taken into consideration. Some of the results are not entirely intuitive, e.g. that the first part of the pipe has initially lower temperature than the downstream parts, but is the last part to be cooled down entirely.

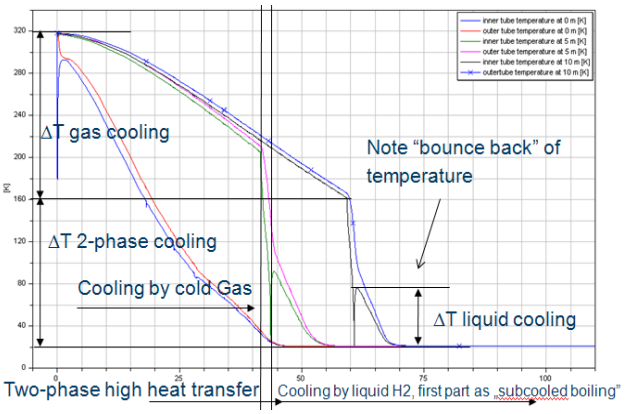

Figure 5: Temperature over time with different phases for a 10m low-pressure pipe during cool down with a hydrogen mass flow of 0.25 kg/s at control valve.

This is explainable from the change of the heat transfer coefficients over time/temperature: obviously the first part of the pipe is cooled down faster at the beginning, but the combination of a cold wall (metal conductivity decreases with temperature) and a low heat transfer coefficient (the beginning of the pipe is exposed to single phase liquid flow at very low Reynolds numbers). This fact, combined with further results omitted here, leads to the result that the cool down time is independent of the pipe length for pipe lengths less than 50 m. The differences between oxygen and hydrogen cool down become clear when looking in more detail at the required energy for the metal cool down and the available specific enthalpy differences for cooling in different phases, tabulated in Table 1. It is obvious that a much larger part of the cooldown is between gas phase and metal for hydrogen, both due to the larger energy content and the larger temperature difference. The gas phase cool down has a lower heat transfer coefficient which

leads to lower stress peaks in the material. Secondly, the rapid cool-down with two-phase flow mostly happens after efficient pre-cooling with cold gas. Overall and against first intuition, cooling down with oxygen poses higher risks in spite of the lower temperature difference. Note also the temperature „bounce-back" of the metal layer in contact with the hydrogen after the hydrogen in the pipe changes from two-phase to liquid. This effect is caused by the drastic drop in heat transfer coefficent in the presence of much warmer outer layers in the pipe metal.

Material / phase	**Energy content for complete cooldown (from 318 K to 80 K for O_2, 20K for H_2)**
Steel 304	101.5 kJ/kg
Steel 316	94.6 kJ/kg
Total Δh H_2	4158 kJ/kg
Total Δh O_2	391.2 kJ/kg
Δh $H_{2\ evap}$	373 kJ/kg
Δh $H_{2\ gas}$	3785 kJ/kg
Δh $O_{2\ evap}$	191.2 kJ/kg
Δh $O_{2\ gas}$	200 kJ/kg

Table 1: Integrated energy content comparison

The largest source of uncertainty in the evaluation of the stress ratio is the occurrence of the „boiling crisis" in two-phase heat transfer at very high heat flow rates. Under such conditions, a thin layer of gas at the metal wall separates the boiling liquid from the metal by an insulating layer, thus drastically reducing the heat flow and the resulting thermal stresses. Correlations for the occurrence of the boiling crisis for cryogenic fluids are not very reliable, data only exists for non-cryogenic fluids. In addition, the boiling crisis condition for cryogenic cooling occurs at (almost) constant temperature of the hot side, which is different form the usual experiments with rapid heating and rising temperature on the hot side.

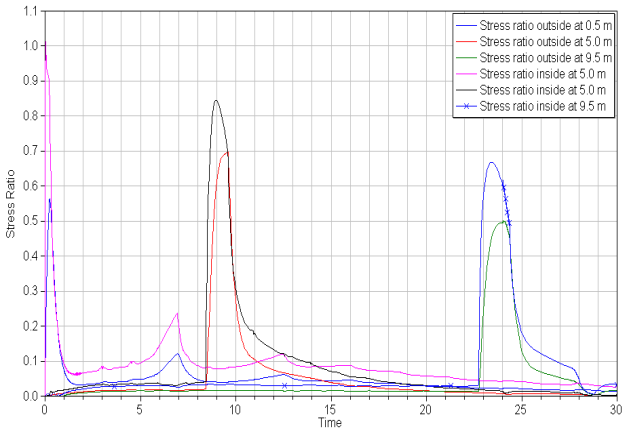

Figure 6: Stress ration along oxygen pipe directly after valve without any pre-cooling.

While this means that the exact heat transfer in the vicinity of the boiling crisis is difficult, the existing correlations can nonetheless be used to estimate the highest reasonable heat transfer coefficient and thus the worst case scenario for the thermal stresses in the metal wall. The results in Figure 6 for a high pressure pipe show that the combination of worst case assumptions (first segments of pipe that is subject to two-phase heat transfer from the start and high coefficinent of heat transfer) lead to stress ratios close to the permissible limit. The stress ratio plot in Figure 6 also shows that locations further downstream are subject to lower stress due to pre-cooling with cold gas. The stress peaks widen and the level decreases as the two-phase zone widens further downstream. A sensitivity study was conducted with repect to the most important parameters for the stress calculation, among others, the heat transfer coefficient, and the result was that the maximum heat transfer coefficient had a negligible effect on the stress ratio. For valves, due to the much thicker metal walls, the stress ratio exceeds 1.0 locally and for brief times. Cryogenic valves survive these conditions, but the high thermal stress leads to local deformations and „cold hardening", but is far from values that would cause complete material failure. While it is not possible to avoid these conditions everywhere in the system, the operation of the plant can be adapted to minimize the number of times and locations that are subject to the extreme conditions. It was, however, possible to avoid the severe thermal stress conditions for valves in the high pressure part of the system.

6 Pipe Bowing

The calculation of the pipe bending due to the temperature difference at the top and bottom of the pipe, when filling with cold liquid, is done with the following assumptions:

- Pipes are considered straight,
- The pipes are fixed at the lower end points with a gliding support at one end to compensate for longitudinal length change,
- Both radial and circumferential heat transfer is taken into consideration in the wall, axial heat transfer is neglected due to axial symmetry.

The liquid cross section area in the pipe is calculated according to *(1)*:

$$A_{liq} = acos\left(1 - \frac{L_{liq}}{r_{pipe}}\right) r_{pipe}^2 + \left(L_{liq} - r_{pipe}\right) \cdot \sqrt{2 \cdot r_{pipe} \cdot L_{liq} - L_{liq}^2} \quad (1)$$

The liquid volume is computed from the mass flow into the horizontal pipe, assumed to end at a closed valve. The mass flow into the pipe is taken from a prior cooldown simulation, at the position of the horizontally connected pipe.

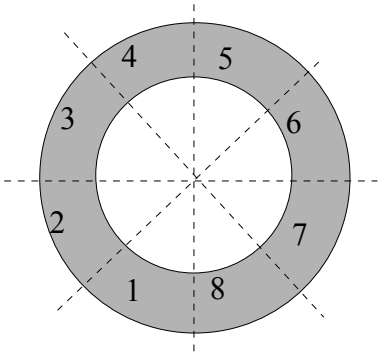

Figure 5: Circumferential discretization of the wall (defined by user)

Simulations use two heat transfer coefficients, one for the part of the wall that is in contact with liquid and the other for the part that is in contact with the gas. The gas temperature has very little influence on the overall result because of the low heat transfer coefficient between gas and pipe wall. Due to the boiling liquid underneath it will within short time after liquid cryogen is at the bottom reach the saturation temperature.

To calculate the heat transfer to the wall the actual liquid level is used to find the length of a discretization that is covered by liquid (if any) and the heat transfer is proportional to this value:

$$\dot{Q} = k_{liq} * \left(T_{wall} - T_{liq}\right) \cdot A_{HT} \cdot \frac{L_{liq} - L_{Dbottom}}{L_{Dtop} - L_{Dbottom}} + k_{gas} \cdot \left(T_{wall} - T_{gas}\right) \cdot A_{HT} \cdot \left(1 - \frac{L_{liq} - L_{Dbottom}}{L_{Dtop} - L_{Dbottom}}\right)$$

where A_{HT} is the heat transfer area, $L_{Dbottom}$ is the length from the bottom of the pipe to the lower boundary of a discretization, L_{Dtop} is the length from the bottom of the pipe to the top boundary of a discretization, k_{liq} is the heat transfer coefficient when in contact with liquid and k_{gas} is the heat transfer coefficient when in contact with the gas. Note that the weighted heat transfer area is a linearization of the inner pipe area fraction around the middle of a circumferential section and should thus only be used for relatively high discretization (16 were considered sufficient).

When calculating the pipe bending only the length change at the top (element 4 and 5 in Figure 5) and bottom (1 and 8 in Figure 5) of the pipe is taken into consideration. The length change is calculated through:

$$\Delta L = L \cdot \alpha\left(T_{wall}\right) \quad (4)$$

where α is the linear expansion coefficient of the material.

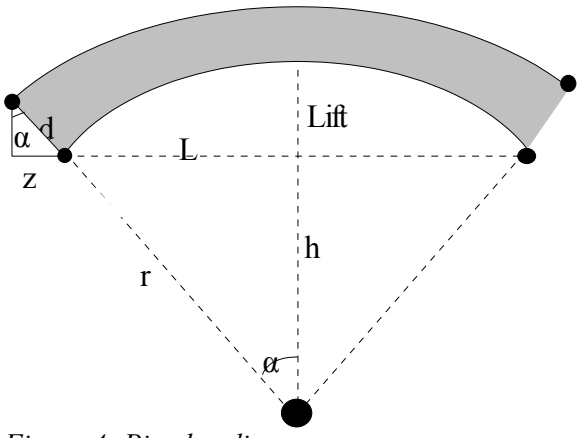

Figure 4: Pipe bending

$$Lift = r - h \quad (5)$$

$$r = \frac{L/2}{\sin(\alpha)} \quad \text{and} \quad \sin(\alpha) = \frac{z}{d} \quad (6)$$

$$h = \frac{L/2}{\tan(\alpha)} \tag{7}$$

(5), *(6)* and *(7)* yields,

$$Lift = \frac{L}{2}\left(\frac{d}{z} - \frac{1}{\tan(\alpha)}\right) \tag{8}$$

If the lift would reach high values of several centimeters, the influence of the lift on the local level and heat transfer would have to be taken into account, but such values are outside of the permissible range anyways.

The worst case encountered in the final modified version of the plant diagram was for a dead end of slighly less than 4 m length and a filling time form empty to full of about 11 minutes. The worst lift was 2.8 cm, a tolerable amount, and the worst case stress ratio using an equivalent stress from the full three-dimensional stress tensor was around 0.45. The length of the pipe has the worst effect on bowing as it effects both the geometry and the exposure time, and dead end pipes longer than 4 m would quickly cause inacceptable bowing.

7 Computational effort

For cooldown scenarios of the larger plant segments, the computational effort was very high: for the most complex segments of the plant cooldown, CPU-times of 3-4 days were necessary for each simulation case, and most of the work is spent during the first few seconds of simulation time. Dymola's version of the dassl solver only managed to survive the initial time without error when the option „equidistant output grid" was switched off. This in turn lead to result files of around 1GB that could not be handled by Dymola and made postprocessing very tedious. Overall, for system simulations of the level of complexity encountered during the cool down simulations, We see the following tool requirements for large scale system simulations with short periods of very sharp gradients:

1. A fine grained control over how many variables are stored and how often they are stored that does not influence the step-size control algorithm. Dymola's Dassl is a bad example of a solver that takes the storage interval into account in a way that lets simulations fail for a small step size to storage interval ratio.
2. Means to influence step size control during extreme gradients under short time, or set a minimum step size and get warnings in the log when the requested accuracy was not achieved.
3. Improved numerical debugging facilities. Dymola's current debugging facilities for numerical problems in large models are insufficient.

8 Conclusions

Modelica is not primarily known for its strength for modeling partial differential equations, but due to its suitability for system level simulations, there are situations in which Modelica and Dymola are an excellent tool even for models that require a full 3-dimensional PDE discretization, under the contraint that this only works for simple geometries. In particular the heat conduction equation with its simple structure can be combined with 1-dimensional two phase flow for thermal stress calculations. The key advantage is that it is possible to capture the most critical thermal stress situation within a complex plant without the need to resort to co-simulation, or difficult to assess assumptions.

This simulation study regarding cool down of a cryogenic transfer system was able to achieve a number of goals, in part because simulation was used already early in the design process:

1. It was possible to establish design guidelines regarding dead pipe ends at closed branches of the network to avoid pipe bowing. The guidelines were incorporated in later revisions of the design.
2. Flow rates were optimized with respect to the contradictory goals of minimum cryogen consumption and avoidance of stratified flow conditions.
3. Simulation results allowed to devise cool down sequences that substantially decreased the thermal stress for all parts in the plant except the parts closest to the tanker used for filling.

There are situations in which there is no possibility to validate simulations against measurements. In spite of that shortcoming, simulation gives important insight into system behaviour and even allows to improve both system design and system operation. Even quantitative analysis is possible to a certain degree when important parameters are well understood and a careful sensitivity analysis is conducted with respect to such parameters.

Cryogenic plant simulations, even under the violent transients that occur during cool down of transfer

lines, can be modeled easily with the cryogenic option of the AirConditioning Library.

References

[1] **Span, R.,** Multiparameter Equations of State. An Accurate Source of Thermodynamic Property Data, Springer, Berlin, 2000.

[2] **Tummescheit, H.:** *Design and Implementation of Object-Oriented Model Libraries using Modelica*, Dissertation, TFRT-1063-SE, Department of Automatic Control, Lund Inst. of Technology, Lund, Schweden, 2002.

[3] **Tummescheit, H., Eborn, J.** und **Prölß, K.:** AirConditioning – a Modelica Library for Dynamic Simulation of AC Systems, in P*roceedings of the 4th International Modelica Conference*, Hamburg, pp. 185 – 192, 2005.

[4] **VDI-Gesellschaft Verfahrenstechnik und Chemiewesen** (Editor), VDI-Wärmeatlas, 9th Edition, Springer, Berlin, 2002

[5] **Versteeg, H. K. and Malalasekera, W**., An Introduction to Computational Fluid Dynamics – The Finite Volume Method, Prentice Hall, 1995.

[6] **Lemmon, E.**, The RefProp User manual, version 7.1, Personal communication See also information on version 7.0 at http://www.nist.gov/srd/nist23.htm (accessed 2005-11-15).

[7] **Fauple J.H.**, **Fisher F.E.**, Engineering Design-A Synthesis of Stress Analysis and Material Engineering, Wiley, New York, 1981.

[8] http://Cryogenics.nist.gov. Accessed October 2005.

[8] **Younglove, B.A.**, Thermophysical Properties of Fluids. I. Argon, Ethylene, Parahydrogen, Nitrogen, Nitrogen Trifluoride, and Oxygen, J. Phys. Chem. Ref. Data, Vol. 11, Suppl. 1, pp. 1-11, 1982.

[9] **D.H. Liebenberg, J.K. Novak, F.J. Edeskuty**: Cooldown of Cryogenic Transfer Systems, AIAA Paper No. 67-475.